

Layered finite element procedure for inelastic analysis of reinforced concrete slabs

Autor(en): **Dotreppe, Jean-Claude / Schnobrich, William C. / Pecknold, David A.**

Objekttyp: **Article**

Zeitschrift: **IABSE publications = Mémoires AIPC = IVBH Abhandlungen**

Band (Jahr): **33 (1973)**

PDF erstellt am: **27.05.2024**

Persistenter Link: <https://doi.org/10.5169/seals-25631>

Nutzungsbedingungen

Die ETH-Bibliothek ist Anbieterin der digitalisierten Zeitschriften. Sie besitzt keine Urheberrechte an den Inhalten der Zeitschriften. Die Rechte liegen in der Regel bei den Herausgebern.

Die auf der Plattform e-periodica veröffentlichten Dokumente stehen für nicht-kommerzielle Zwecke in Lehre und Forschung sowie für die private Nutzung frei zur Verfügung. Einzelne Dateien oder Ausdrucke aus diesem Angebot können zusammen mit diesen Nutzungsbedingungen und den korrekten Herkunftsbezeichnungen weitergegeben werden.

Das Veröffentlichen von Bildern in Print- und Online-Publikationen ist nur mit vorheriger Genehmigung der Rechteinhaber erlaubt. Die systematische Speicherung von Teilen des elektronischen Angebots auf anderen Servern bedarf ebenfalls des schriftlichen Einverständnisses der Rechteinhaber.

Haftungsausschluss

Alle Angaben erfolgen ohne Gewähr für Vollständigkeit oder Richtigkeit. Es wird keine Haftung übernommen für Schäden durch die Verwendung von Informationen aus diesem Online-Angebot oder durch das Fehlen von Informationen. Dies gilt auch für Inhalte Dritter, die über dieses Angebot zugänglich sind.

Layered Finite Element Procedure for Inelastic Analysis of Reinforced Concrete Slabs

Analyse non-élastique par couches de plaques en béton armé selon la méthode des éléments finis

Nichtelastische, schichtweise Berechnung von Stahlbetonplatten nach der Methode der endlichen Elemente

JEAN-CLAUDE DOTREPPE

University of Liège, Liège, Belgium

WILLIAM C. SCHNOBRICH

DAVID A. PECKNOLD

University of Illinois at Urbana-Champaign, Urbana, Illinois 61801 USA

Introduction

The development of numerical procedures for the post-elastic stress analysis of reinforced concrete plates and shells is a research area currently receiving a good deal of attention. The central difficulty in evolving such procedures concerns development of incremental relations between stress resultants and strain measures which, though idealized, adequately reflect cracking, yielding and crushing of concrete and yielding of steel reinforcement. Once such relations have been obtained, standard numerical techniques such as the finite element method, can be employed to trace out the desired (nonlinear) load-deflection response of the structure.

In the past, two distinctly different viewpoints have been taken in an effort to obtain the necessary constitutive relations. In the first approach, exemplified by the work of JOFRIET and MCNEICE [5] and BELL [2], a semi-empirical overall moment-curvature relation is employed which attempts to take into consideration the various stages of material behavior. In the second approach, the incremental constitutive relations for the composite structure are synthesized from the corresponding relations for the individual constituents, concrete and steel. CERVENKA [3] took the latter avenue in his study of reinforced concrete panels subjected to inplane loading. In order to consider

flexural deformation, the variation of material properties through the thickness must be accounted for. This can be done by means of a layering approach or by the introduction of numerical integration points through the thickness. The layering concept was applied by WHANG [11] to the elastoplastic analysis of shells, and is a physically interpretable special case of the integration point approach suggested by MARCAL [8]. HAND [4], in work completed subsequent to that reported here, employed the layering approach to develop an analysis procedure for reinforced concrete plates and shells.

A rather interesting phenomenon often occurs after cracking has taken place in the structure. The constitutive relations exhibit coupling between membrane and flexural effects, similar to that which occurs in unsymmetrically laminated plates. A consequence of this fact is that the inplane and plate bending problems no longer uncouple, and membrane boundary conditions must be specified. The practical significance of this observation remains an open question, but HAND [4] has shown that inplane boundary conditions can have a large effect on computed load deflection histories. In the literature on the analysis of laminated plates, the "reduced bending stiffness" approximation, equivalent to assuming the membrane stress resultants to be zero, is often used [1], [9]. This assumption "approximately" uncouples the problem and allows a corresponding reduction in computational effort. In much of the reported work on reinforced concrete plates the same approximation is employed either implicitly or explicitly [10]. The general validity of such an approach requires further investigation.

In this paper a finite element approach for the post-elastic stress analysis of reinforced concrete plates under monotonically increasing load is described. Concrete is assumed to be brittle in tension and to yield in biaxial compression according to the yield criterion of KUPFER, HILSDORF and RUSCH [6]. Reinforcing steel is assumed to be elastic-perfectly plastic. The layering approach is employed, in conjunction with a twelve-degree-of-freedom plate bending finite element. An approximation, essentially the "reduced bending stiffness" approximation, is employed, so that the number of degrees of freedom can be reduced from five to three per node. The adequacy of this approximation is discussed in the context of two particular numerical examples. In the first example, comparisons are made, both with experimental results, and with the results of HAND [4], who included inplane degrees of freedom in his analysis.

Material Properties

The objective is to obtain appropriate incremental relations between stress resultants and the midsurface strains and curvatures of the plate for use in a finite element procedure. To accomplish this, attention is first focused on a thin lamina at a distance z from, and parallel to, the plate midsurface. As is

usual in thin plate theory, the assumption is made that each such lamina is in a state of plane stress. In this section the incremental stress-strain relations for the lamina are obtained. In the following section these relations are utilized to develop the desired relations between stress resultants and midsurface strains and curvatures.

The incremental stress-strain relations for the lamina can be expressed in the form

$$\{\Delta \sigma\} = [C]\{\Delta \epsilon\}, \quad (1)$$

where $\{\Delta \sigma\} = \{\Delta \sigma_x, \Delta \sigma_y, \Delta \tau_{xy}\}^T$, $\{\Delta \epsilon\} = \{\Delta \epsilon_x, \Delta \epsilon_y, \Delta \gamma_{xy}\}^T$,

by requiring complete deformation compatibility between concrete and steel. In (1), $\{\Delta \sigma\}$ represents an increment of pseudo-stress,

$$\{\Delta \sigma\} = \sum_i \mu^i \{\Delta \sigma\}^i, \quad (2)$$

where $\{\Delta \sigma\}^i$ is the stress increment in the i^{th} constituent¹⁾, and μ^i is the area ratio of the i^{th} constituent. Thus $[C]$ is defined in terms of the incremental material property matrices $[C]^i$ of the constituents by

$$[C] = \sum_i \mu^i [C]^i. \quad (3)$$

The nature of the matrices $[C]^i$ of course depends on the idealizations of material behavior. These are discussed below.

Concrete is idealized as a tension-limited elastic perfectly plastic material. The corresponding uniaxial stress-strain curve is shown in Fig. 1. In order to generalize this to biaxial states of stress, an appropriate yield criterion is needed. In this study, the yield criterion of KUPFER, HILSDORF and RUSCH [6],

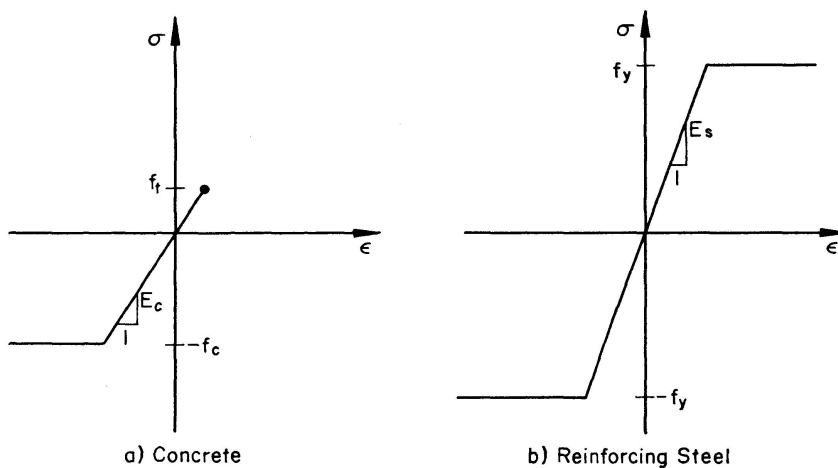


Fig. 1. Idealized uniaxial stress-strain curves for concrete and steel.

¹⁾ The constituents considered here are concrete and the steel reinforcement. A superscript "c" denotes concrete, "s" denotes steel.

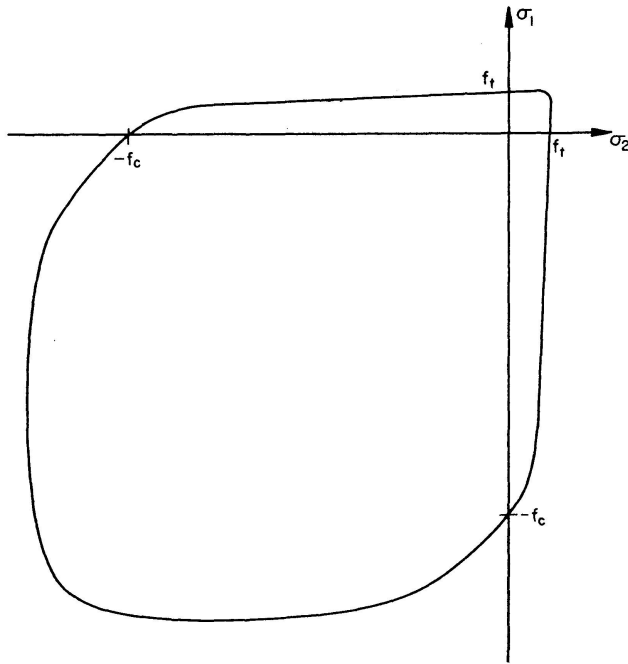


Fig. 2. Concrete biaxial yield criterion of KUPFER, HILSDORF and RUSCH.

which is based on experimental results, is employed (Fig. 2). The procedure for adapting the Kupfer, Hilsdorf and Rusch criterion to the incremental analysis is fully discussed in [13]. The criterion obtained is of the form

$$\tau_{oct} = a - b p, \quad (4)$$

where τ_{oct} is the octahedral shearing stress in the concrete,

p is the mean stress in the concrete,

a, b are material constants which take different values depending on the signs of the concrete principal stresses.

The criterion (4) is employed to detect both cracking and biaxial yielding of the concrete. When cracking occurs, the cracks are assumed to be perpendicular to the concrete principal tensile stress. The corresponding material property matrix in a coordinate system aligned with the cracks is

$$[\bar{C}]^c = E_c \begin{bmatrix} 1 & 0 & 0 \\ 0 & 0 & 0 \\ 0 & 0 & 0 \end{bmatrix}, \quad (5)$$

where E_c is the modulus of elasticity of the concrete. A coordinate transformation produces the desired matrix in the (x, y) system.

In (5) it is tacitly assumed that the cracked concrete can carry no shear. HAND [4] has indicated the desirability of incorporating a "shear retention" factor in (5) to compensate for phenomena such as aggregate interlock and dowel action which have been neglected in the mathematical idealization. A related concept has been employed by SCANLON [10].

In the plastic range, the concrete incremental stress-strain relations are

obtained in the usual way, by requiring the incremental plastic strain vector to be normal to the yield surface.

The result is

$$[C]_{ep}^c = [C]_{el}^c - \frac{[C]_{el}^c \hat{n} \hat{n}^T [C]_{el}^c}{\hat{n}^T [C]_{el}^c \hat{n}}, \quad (6)$$

in which $[C]_{ep}^c$ is the concrete incremental stress-strain matrix in the plastic range,

$[C]_{el}^c$ is the concrete incremental stress-strain matrix in the elastic range,

and \hat{n} is the unit normal to the yield surface at the current state of stress.

The reinforcing steel is assumed to be elastic perfectly plastic, and is in a state of uniaxial stress. The corresponding stress-strain curve is shown in Fig. 1.

Constitutive Relations for Layered Plate

In the previous section incremental stress-strain relations for a lamina in plane stress were developed. The variation in material properties through the thickness is discretized by dividing the plate into layers (Fig. 3), within each

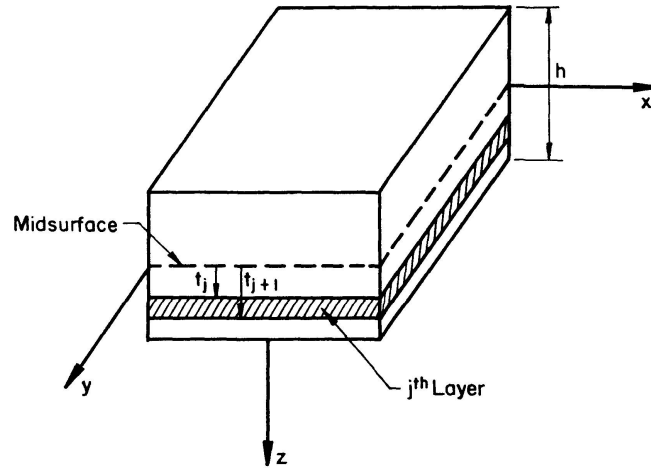


Fig. 3. Layered plate.

of which the material properties are constant²⁾. Thus, the incremental stress-strain relations for the lamina become

$$\{\Delta \sigma\} = [C]_j \{\Delta \epsilon\}, \quad (7)$$

where the subscript j now identifies the layer in which the lamina is located. The Kirchhoff assumption

$$\{\Delta \epsilon\} = \{\Delta \epsilon_0\} + z \{\Delta K\} \quad (8)$$

²⁾ The material properties for the entire layer are taken to be those at mid-layer.

and the definition of the stress resultants,

$$(\{\Delta N\}, \{\Delta M\}) = \int_{-h/2}^{h/2} (1, z) \{\Delta \sigma\} dz \quad (9)$$

yield the desired constitutive relations

$$\begin{Bmatrix} \Delta N \\ \Delta M \end{Bmatrix} = \begin{bmatrix} D_{11} & D_{12} \\ D_{21} & D_{22} \end{bmatrix} \begin{Bmatrix} \Delta \epsilon_0 \\ \Delta K \end{Bmatrix}. \quad (10)$$

In these equations, $\{\Delta \epsilon_0\}, \{\Delta K\}$ are the 3×1 vectors of midsurface strain and curvature, respectively, and

$$\{\Delta N\} = \{\Delta N_x, \Delta N_y, \Delta N_{xy}\}^T, \{\Delta M\} = \{\Delta M_x, \Delta M_y, \Delta M_{xy}\}^T.$$

The 3×3 material property matrices in (10) are

$$\begin{aligned} [D_{11}] &\equiv \sum_j (t_{j+1} - t_j) [C]_j, \\ [D_{12}] = [D_{21}]^T &\equiv \sum_j \frac{(t_{j+1}^2 - t_j^2)}{2} [C]_j, \\ [D_{22}] &\equiv \sum_j \frac{(t_{j+1}^3 - t_j^3)}{3} [C]_j, \end{aligned} \quad (11)$$

where t_j and t_{j+1} are the distances from the midsurface to the top and bottom, respectively, of the j^{th} layer (Fig. 3).

Unless the section possess material property symmetry about the midsurface the matrices $[D_{12}]$, $[D_{21}]$ in (10) are non-zero. Even if this were the case initially, cracking and yielding would eventually destroy such symmetry.

Thus coupling is produced between membrane and flexural effects, with the result that even for plates loaded only in the transverse direction, inplane boundary conditions are required. The quantitative influence of the inplane conditions may not be large however, and in order to reduce computational effort the "reduced bending stiffness" approximation is introduced. It is assumed that the inplane stress resultants $\{N\}$ are zero. Thus, in terms of incremental quantities, (10) yields

$$\{\Delta \epsilon_0\} = -[D_{11}]^{-1} [D_{12}] \{\Delta K\}. \quad (12)$$

The incremental bending moments are then given by

$$\{\Delta M\} = [D^*] \{\Delta K\}, \quad (13)$$

where $[D^*] \equiv [D_{22}] - [D_{21}][D_{11}]^{-1}[D_{12}]$ is the "reduced bending stiffness". This approximation can be viewed as a transformation such that the moments are computed with respect to a "generalized neutral surface", analogous to the neutral axis in reinforced concrete beams. Strictly speaking, a neutral surface does not exist in general, if by neutral surface is meant a surface on which all membrane strains are zero. Nevertheless, the foregoing interpretation is useful.

For later reference the incremental bending moments appearing in (13) are rewritten in terms of stresses integrated through the plate thickness as

$$\{\Delta M\} = \int_{-h/2}^{h/2} [z[I] - [D_{21}][D_{11}]^{-1}]\{\Delta \sigma\} dz. \quad (14)$$

Eq. (14) reduces to the definition (9) since $\{\Delta N\} = 0$. This merely expresses the fact that the bending moment is the same with respect to all reference surfaces in the absence of a resultant force.

The incremental stiffness matrix for the plate finite element is formed using the "reduced bending stiffness" $[D^*]$. The resulting expression is

$$[K] = \int_A [B]^T [D^*] [B] dA \quad (15)$$

where $[B]$ is the usual 3×20 matrix relating curvatures to element nodal displacements. A description of the standard twelve degree-of-freedom plate bending finite element used may be found in ZIENKIEWICZ [12].

As, in general, a neutral surface does not exist, a slightly modified version of the foregoing procedure was employed. The modification is based on the physical interpretation of the "reduced bending stiffness" approximation. In place of (12), the expression

$$\{\Delta \epsilon_0\} = -[\alpha]\{\Delta K\} \quad (16)$$

was used, where

$$[\alpha] \equiv \begin{bmatrix} \alpha_x & 0 & 0 \\ 0 & \alpha_y & 0 \\ 0 & 0 & \alpha_{xy} \end{bmatrix}. \quad (17)$$

Eq. (16) represents a shift of reference surface such that ΔM_x is computed about a surface on which $\Delta \epsilon_x = 0$, ΔM_y about a surface on which $\Delta \epsilon_y = 0$, and ΔM_{xy} about a surface on which $\Delta \gamma_{xy} = 0$. The three quantities α_x , α_y , α_{xy} are not independent because of Saint Venant's well-known compatibility equation between ϵ_x , ϵ_y , ϵ_{xy}

$$\frac{\partial^2 \epsilon_x}{\partial y^2} + \frac{\partial^2 \epsilon_y}{\partial x^2} = \frac{\partial^2 \gamma_{xy}}{\partial x \partial y}.$$

The corresponding definition of the transformed incremental moments, similar to (14), is

$$\{\Delta M\} = \int_{-h/2}^{h/2} [z[I] - [\alpha]]^T \{\Delta \sigma\} dz \quad (19)$$

and the approximate incremental bending stiffness is

$$[D^*]_{app} = \sum_j \int_{t_j}^{t_{j+1}} [z[I] - [\alpha]]^T [C]_j [z[I] - [\alpha]] dz, \quad (20)$$

which can be rewritten as

$$[D^*]_{app} = [D_{22}] - [\alpha]^T [D_{12}] - [D_{21}][\alpha] + [\alpha]^T [D_{11}][\alpha]. \quad (21)$$

Note that if $[\alpha] = [D_{11}]^{-1}[D_{12}]$, the right hand side of (21) reduces to $[D^*]$. In order to gain some insight into the nature of the approximations, consider a loading increment during which the material properties do not change. If those cases are excluded in which nonzero boundary rotations or displacements are imposed the "reduced bending stiffness" approximation produces a "softer" structure than is actually the case³). This can be shown by the principle of minimum complementary energy since the approximation is a statically admissible field. The effect of the further approximation, Eqs. (16) to (21), can be shown by defining $[E] \equiv [\alpha] - [D_{11}]^{-1}[D_{12}]$. Eq. (21) then becomes

$$[D^*]_{app} = [D^*] + [E]^T [D_{11}] [E]. \quad (22)$$

Since $[D_{11}]$ is positive definite, $[E]^T [D_{11}] [E]$ is positive semi-definite at least, and the further approximation "stiffens" the structure, and thus perhaps partly cancels the softening effect of the first approximation.

Numerical Procedure

The external loading is applied in increments (Fig. 4). At the beginning of each load increment the structure tangent stiffness matrix is updated to reflect any changes in material properties which have taken place. Inelastic action within the load increment is taken into account by the "initial stress" method [12], in which pseudo-loads reflecting the inelastic behavior are iteratively redistributed through the structure using the tangent stiffness computed at the beginning of the increment. This procedure is quite efficient and requires the use of relatively few load increments.

For the i^{th} load increment $\{\Delta P\}_i$, the first approximation to the incremental displacements are calculated from

$$[K]_i \{\Delta U\}_i^{(0)} = \{\Delta P\}_i \quad (23)$$

using the tangent stiffness $[K]_i$.

Subsequent iterations take the form

$$[K]_i \{\Delta U\}_i^{(r+1)} = \{\Delta P\}_i^{(r)}, \quad (24)$$

where $\{\Delta P\}_i^{(r)}$ is the structure pseudo-load vector reflecting additional inelastic action due to the displacement increment $\{\Delta U\}_i^{(r)}$. The total incremental displacement for the i^{th} load increment (after N iterations) is then given by

$$\{\Delta U\}_i = \sum_{n=0}^N \{\Delta U\}_i^{(n)}. \quad (25)$$

³) These considerations are quite apart from approximations made in the finite element discretization of the structure.

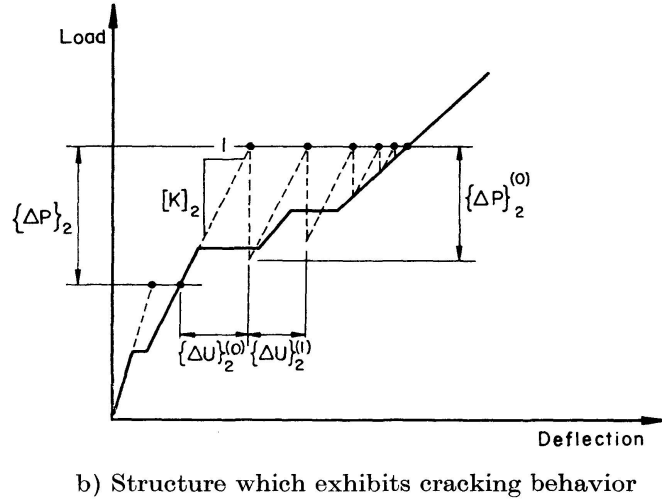
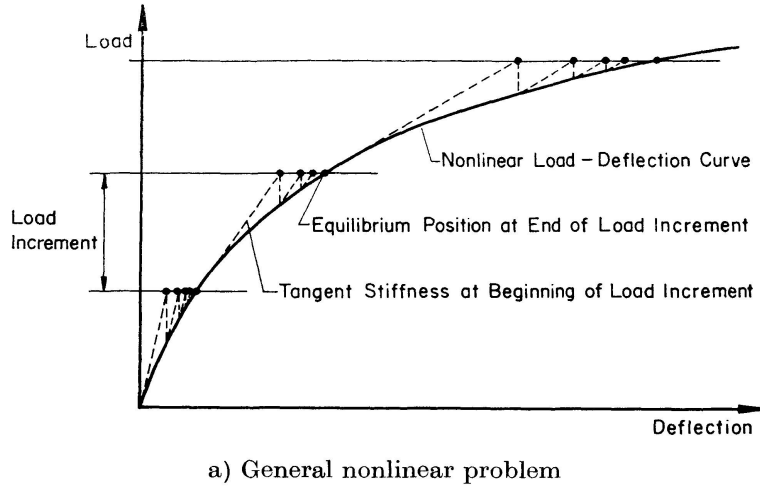


Fig. 4. Schematic diagram of combined "tangent stiffness-initial stress" numerical procedure.

The structure pseudo-load vector, $\{\Delta P\}_i^{(r)}$, appearing in (24) is assembled from the element pseudo-load vectors in the conventional manner.

Although the approximation $\{\Delta N\} = 0$ has been made, membrane forces appear during the iteration process since the intermediate configurations (Fig. 4) are not equilibrium states. Thus the element pseudo-load vector must take into account excess membrane forces as well as bending moments. If the excess stress resultants for a given element are denoted by

$$\begin{Bmatrix} \Delta \tilde{N}_i^{(r)} \\ \Delta \tilde{M}_i^{(r)} \end{Bmatrix}$$

the element pseudo-load vector is given by

$$\{\Delta P\}_i^{(r)} = \int_A [B]^T \{ \{\Delta \tilde{M}\}_i^{(r)} - [D_{21}][D_{11}]^{-1} \{\Delta \tilde{N}\}_i^{(r)} \} dA \quad (26)$$

$$\text{or} \quad \{\Delta P\}_i^{(r)} = \int_A [B]^T \{ \{\Delta \tilde{M}\}_i^{(r)} - [\alpha]^T \{\Delta \tilde{N}\}_i^{(r)} \} dA \quad (27)$$

depending on which of the two approximations described earlier is used, where $[D_{11}]$, $[D_{12}]$, $[\alpha]$ are evaluated at the beginning of the increment.

When the concrete is in the plastic range, the stress point tends to gradually drift off the yield surface since in this case the incremental relations are valid only for infinitesimal increments. To counteract this effect, after each iteration the stress point is drawn back to the yield surface along a ray passing through the origin. It is noted that it may be preferable to make this correction along an "average"⁴⁾ normal to the yield surface, but this refinement has not been employed here.

Examples

1. Corner-Propped Slab

To demonstrate the accuracy of the numerical results which can be obtained from the described procedure, the corner-propped slab of JOFRIET and MCNEICE [5] was analyzed. The slab was 36 inches square, 1.75 inches thick, and was reinforced with an isotropic mesh of 0.85% reinforcing steel. The loading consisted of a central concentrated load. Fig. 5 shows the grid used in the finite element solution, together with the relevant material property data. Six layers through the plate thickness were used and the load was applied in 400 lb increments. Fig. 6 shows the computed deflection history at a particular node together with experimental results. The agreement is quite good, although a trend begins to appear in the later stages of loading in which the computed results are somewhat "stiffer" than the observed. The discrepancy is not

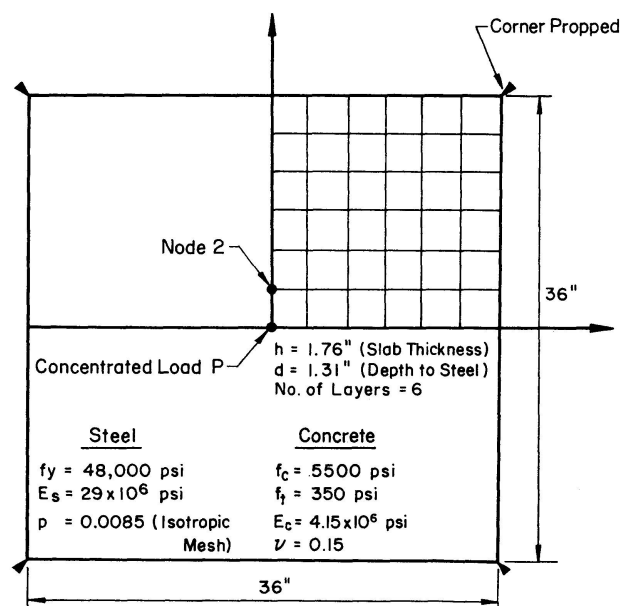


Fig. 5. Material properties and finite element mesh for corner-propped slab.

⁴⁾ Some weighted average of the normals at the beginning and end of the increment.

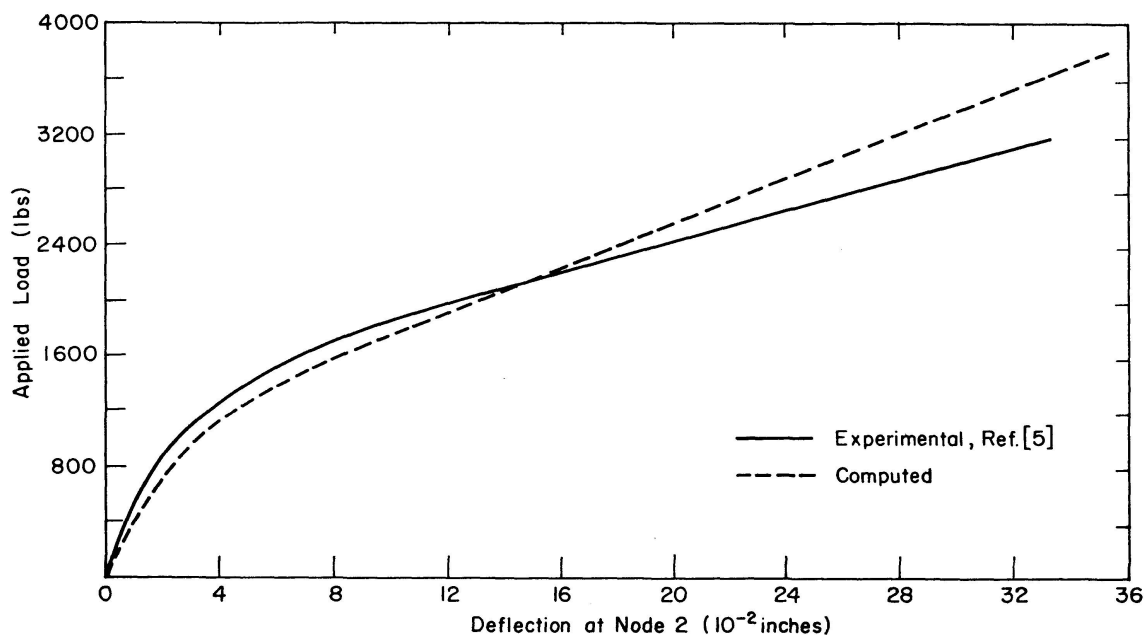


Fig. 6. Computed and experimental load-deflection responses of corner-propped slab.

serious, the computed deflections being on the order of 15% too low at quite high loads. It might be speculated that the stiffening effect of the second approximation discussed earlier is beginning to be felt as cracking becomes more severe. HAND [4] applied the same layering approach to reinforced concrete plates and shells, where he included inplane degrees of freedom. He calculated the same example for two different membrane boundary conditions, one in which the corner pins are rigid inplane and the second in which they

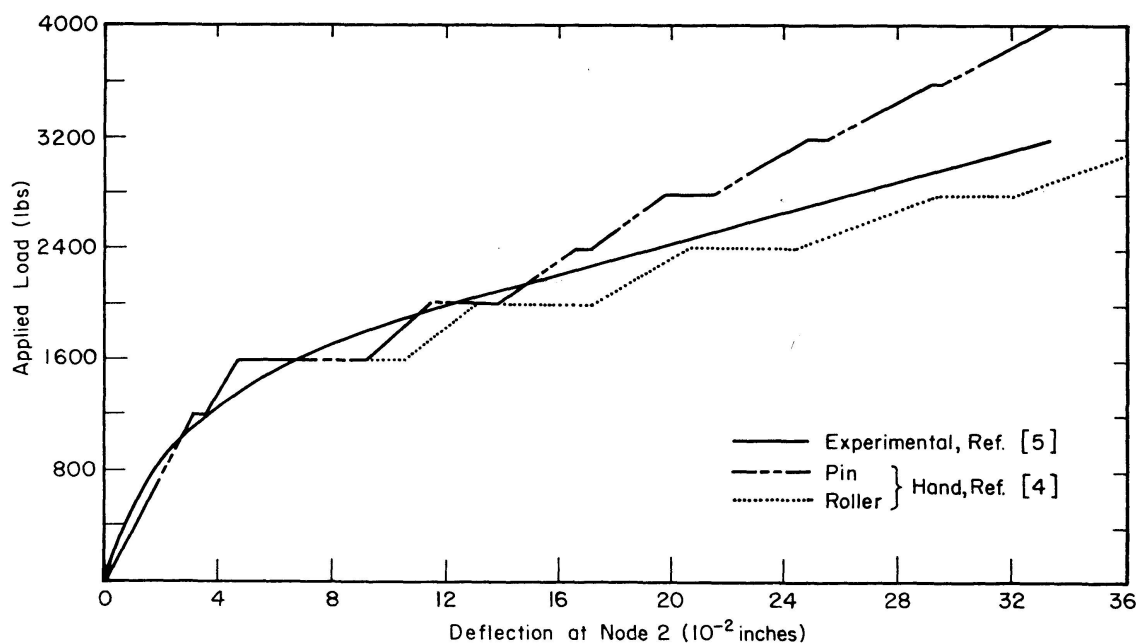


Fig. 7. Effect of inplane boundary conditions on computed deflections of corner-propped slab (after HAND, ref. [4]).

are on rollers. Fig. 7 shows the results he obtained. The difference between the two computed load-deflection curves is surprising, and it is noted that they bound the computed curve shown in Fig. 6. Since it is uncertain what the inplane boundary conditions were in the actual test, and since the computed results are within the probable variability due just to a change of membrane boundary conditions, the accuracy of the results presented here is judged to be satisfactory. Others [7], [10], including JOFRIET and MCNEICE [5], have analyzed this slab, however no comparison of the various numerical solutions is undertaken here. Further comparisons for a variety of situations are required before any judgements can be made regarding the superiority of one procedure over another, although the results presented here do compare favorably with these other numerical solutions for this particular case.

2. Simply Supported Slab

Another example is presented here, which is taken from tests performed by the Portland Cement Association in 1954. Results for this test may be found in reference [14].

The slab is 72 inches square, 5.5 inches thick and is reinforced with an isotropic mesh of 0.99% reinforcing steel (Fig. 8). The load is centrally applied on a small column cast integrally with the slab as is also shown in Fig. 8.

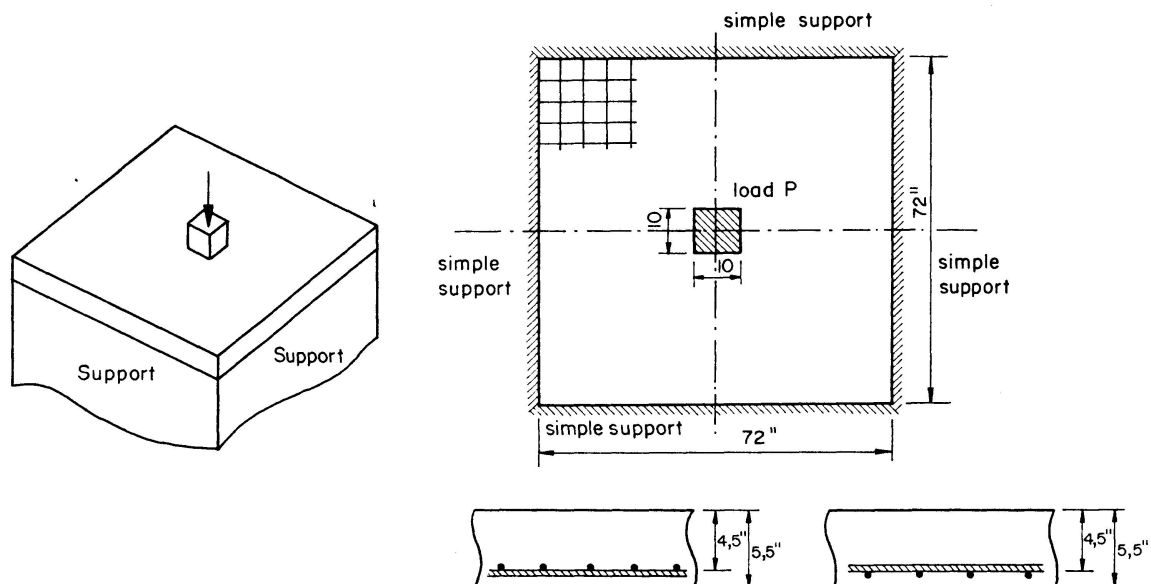


Fig. 8. Loading system and reinforcement mesh for simply supported square slab.

Fig. 9 shows the grid used in the finite element solution, together with the material properties. Again six layers were used and the load was applied in 8000 lb increments.

Fig. 10 shows the comparison between experimental and theoretical results for the load-deflection curve at the center of the plate. Again there is a good

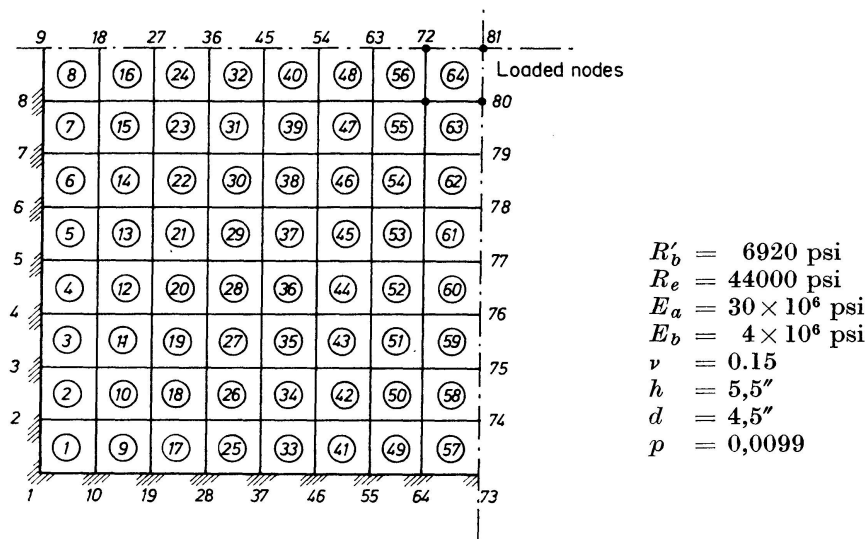


Fig. 9. Finite element mesh and material properties for simply supported slab.

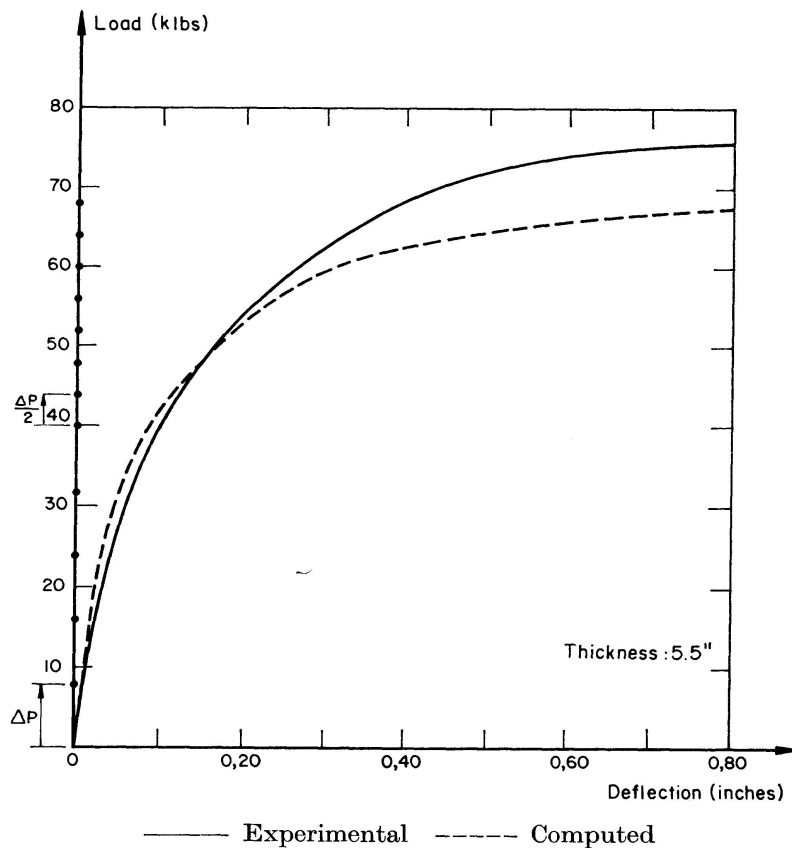


Fig. 10. Theoretical and experimental load-deflection curves at the center of the plate.

agreement except near failure. According to Hand's results, this might be due to the coupling between membrane and flexural effects as explained before. The discrepancy is small, however; the computed failure load is only on the order of 10% too low. Fig. 11 shows some interesting results which can

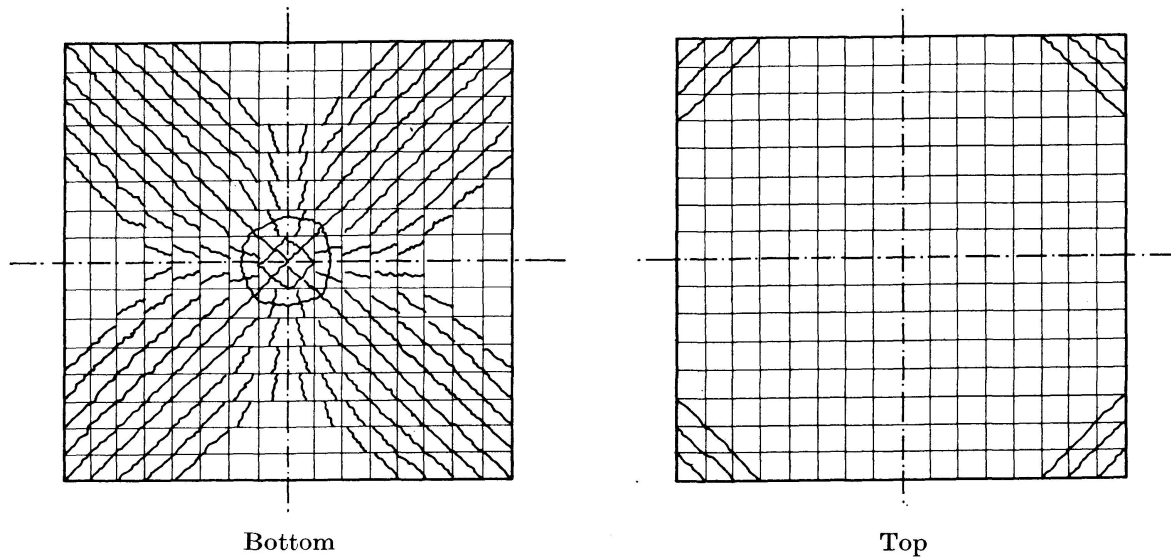


Fig. 11. Theoretical cracking patterns at bottom and top faces for the simply supported square slab.

be obtained directly from the program, i. e. cracking patterns at the bottom and the top of the plate. Those results also compare favorably with experimental cracking patterns of similar types of plates.

Conclusions

A numerical procedure has been presented which is capable of tracing out the post-elastic load deflection behavior of reinforced concrete plates under monotonically increasing loading as well as theoretical cracking patterns. Cracking and yielding of concrete and yielding of steel reinforcement are incorporated in the mathematical model. Approximations which allowed a significant reduction in computational effort were made, and their effects were discussed qualitatively and, in the context of two examples, quantitatively. It is felt that the procedure described here provides results of reasonable accuracy, but further study of the effects of inplane boundary conditions is needed.

Acknowledgment

This investigation was carried out as part of a research program in the Department of Civil Engineering of the University of Illinois at Urbana-Champaign, and was sponsored by the National Science Foundation under Grant No. NSF GK 11190.

References

1. J. E. ASHTON: Approximate Solutions for Unsymmetrically Laminated Plates. *J. Composite Materials*, Vol. 3, 1967, p. 189.
2. J. C. BELL: A Complete Analysis for Reinforced Concrete Slabs and Shells. Ph. D. Thesis, Univ. of Canterbury, Christchurch, New Zealand, 1970.
3. V. CERVENKA: Inelastic Finite Element Analysis of Reinforced Concrete Panels Under Inplane Loads. Ph. D. Thesis, Univ. of Colorado, Boulder, Colorado, 1970.
4. F. R. HAND, D. A. PECKNOLD, and W. C. SCHNOBRICH: Layered Finite Element Nonlinear Analysis of Reinforced Concrete Plates and Shells. Structural Research Series No. 389, Department of Civil Engineering, Univ. of Illinois at Urbana-Champaign, Urbana, Ill., August, 1972.
5. J. C. JOFRIET and G. M. MCNEICE: Finite Element Analysis of Reinforced Concrete Slabs. *J. Structural Div., ASCE*, Vol. 97, No. ST 3, March 1971, p. 785.
6. H. KUPFER, H. K. HILSDORF and H. RUSCH: Behavior of Concrete Under Biaxial Stresses. *J. American Concrete Inst.*, Vol. 66, No. 8, Aug. 1969, p. 656.
7. C. S. LIN: Nonlinear Analysis of Reinforced Concrete Slabs and Shells. Ph. D. Thesis, Univ. of California, Berkeley, Calif. (to be submitted in Sept. 1972).
8. P. V. MARCAL: Finite Element Analysis with Material Nonlinearities – Theory and Practice. Recent Advances in Matrix Methods of Structural Analysis and Design, ed. by R. H. Gallagher, Y. Yamada and J. T. Oden, Univ. of Alabama Press, 1971.
9. E. REISSNER and Y. STAVSKY: Bending and Stretching of Certain Types of Heterogeneous Anisotropic Elastic Plates. *J. Applied Mechanics*, Vol. 28, 1961, p. 402.
10. A. SCANLON: Time Dependent Deflections of Reinforced Concrete Slabs. Ph. D. Thesis, Univ. of Alberta, Edmonton, Canada, 1971.
11. B. WHANG: Elastic-Plastic Orthotropic Plates and Shells. Application of Finite Element Methods in Civil Engineering, Vanderbilt University, Nashville, Tenn., Nov. 1969.
12. O. C. ZIENKIEWICZ: The Finite Element Method in Engineering Science. McGraw-Hill, 1971.
13. M. J. MIKKOLA, and W. C. SCHNOBRICH: Material Behavior Characteristics for Reinforced Concrete Shells Stressed Beyond the Elastic Range. Structural Research Series No. 367, Department of Civil Engineering, Univ. of Illinois at Urbana-Champaign, Urbana, Illinois, August 1970.
14. C. ELSTNER and E. HOGNESTAD: Shearing Strength of Reinforced Concrete Slabs. *Journal of the American Concrete Institute*, Vol. 28, No. 1, July 1956.

Summary

A non-linear finite element procedure is presented for the inelastic stress analysis of reinforced concrete slabs including the effects of cracking, yielding of concrete and yielding of reinforcing steel. Material property variation through the slab thickness is accounted for in discretized fashion by means of a layering approach. Approximations are discussed which reduce the effects of membrane-flexure coupling in the constitutive equations due to inelastic action, and thus allow a reduction in computational effort. A comparison is

made between computed and experimental results for two centrally loaded plates: one is a corner-propped slab, the other is simply supported along the four edges.

Résumé

On décrit une méthode de calcul par éléments finis des dalles en béton armé jusqu'à la ruine, et en particulier dans la phase non-linéaire: on examine l'influence de la fissuration, de la plastification du béton ainsi que de la plastification des barres d'armature. On tient compte de la variation des propriétés du matériau sur l'épaisseur de la plaque en divisant celle-ci en couches de propriétés différentes. On introduit certaines approximations qui réduisent, dans les équations constitutives, le couplage entre les effets flexionnels et les effets membranaires. On présente une comparaison entre résultats théoriques et expérimentaux pour deux plaques chargées au centre: l'une est appuyée aux quatre coins, l'autre est simplement appuyée le long des quatre bords.

Zusammenfassung

Ein nichtlineares Finite-Element-Verfahren für die nichtelastische Stressanalyse von Eisenbetonplatten wird beschrieben, das die Effekte von Rissbildung, Versagen des Betons und Versagen des Stahls mit einschliesst. Die Änderung der Materialeigenschaften über die Plattendicke wird in diskretisierter Weise durch Einführung von Schichten berücksichtigt. Näherungen werden diskutiert, welche die Wirkung der Koppelung zwischen Scheiben- und Plattenwirkung infolge nichtelastischen Verhaltens vereinfachen und dadurch eine Reduktion des Computeraufwandes erlauben. Es wird ein Vergleich der gerechneten und experimentell gewonnenen Resultate für zwei zentrisch belastete Platten vorgenommen: die eine ist an den Ecken gestützt, die andere entlang den vier Rändern einfach gelagert.